An Experimental High Precision GNSS Receiver for Small Satellites Navigation

Juan G. Díaz, G. Ramón López La Valle, Santiago Rodríguez, Germán Scillone, Lucas Mártire, Ernesto M. López, Gerardo L. Puga, Jorge Cogo, Javier A. Smidt, Javier G. García, and Pedro A. Roncagliolo

Grupo SENyT – Facultad de Ingeniería – Universidad Nacional de La Plata
Calle 116 y 48, 1900 La Plata, Argentina
Phone: +54 221 4259306, Mail: agustinr@ing.unlp.edu.ar

Abstract: A new GNSS receiver intended for small satellite applications, completely designed and built in Argentina, is presented in this work. The different aspects of its architecture and design are presented, as well as the first experimental results obtained with a prototype of the GNSS receiver and a GNSS signal simulator. These tests show the excellent quality of the raw measurements produced, which are on a par with the best modern high-precision GNSS receivers and clearly indicate the high potential of the receiver for absolute and relative orbit determination.

1. INTRODUCTION

The use of Global Navigation Satellite Systems (GNSS) in Low Earth Orbit (LEO) satellites is a widely adopted solution for on-board orbit determination, as long as the weight, volume and power consumption of the receiver is compatible with the mission budget. The demanding conditions of the space environment, i.e. vacuum, thermal cycling and high energy radiation, often lead to bigger, with more power consumption, and much more expensive receivers. For these reasons, the usual space qualified GNSS receivers are typically not an option for many small satellite missions. Nowadays, the distributed system approach -which replaces big satellite solutions by many small cooperative satellites- is increasing the previous constrains, but also requiring more accurate positioning abilities. In particular, the need of highly accurate relative positioning between the elements of a distributed earth observation instrument is one of the key aspects of this approach.

In this work we present a GNSS demonstration receiver that, being compatible with usual small satellites constrains, can provide very accurate raw measurements - i.e. pseudoranges and carrier phase - which in turn enable the use of highly precise absolute and relative positioning techniques. The receiver architecture allows receiving any two GNSS bands selected by the user, i.e. GPS L1 and GLONASS L1 or GPS L1 and GPS L2, and it is designed without relying on integrated circuits that often do not have qualified counterparts and that typically limit the signal bandwidth. This latter limitation makes them inadequate for high precision measurements receivers. The same philosophy is adopted for the digital part of the receiver, which in particular is based on

a Field Programmable Gate Array (FPGA) -with military grade version- on wich an embedded processor and a correlation system is implemented using Hardware Description Language, without any dependence on Intellectual Property (IP) Cores. In this way, the receiver design can be tailored according the quality parts policy of a particular mission. Regarding the software, it's implemented using a real-time operating system, and it has four main parts: satellite signal acquisition, satellite signal tracking, satellite raw signal measurements generation, and lastly Position, Velocity and Time (PVT) calculation. In this last part, an Extended Kalman Filter (EKF) based on the required dynamic orbit model can be implemented to provide an adequate dynamic filtering to the navigation solution.

The rest of the paper is organized as follows: In Section 2 the receiver hardware architecture, design and implementation is described. The digital processing stage implemented into the FPGA is described in Section 3 and the software structure is briefly presented in Section 4. Experimental tests that determine the raw measurements performance of the receiver are presented in Section 5. These results show that the pseudorange error is less than 12cm, and that the carrier phase error is less than 0.7mm, values which are nowadays only attainable by a few high precision GNSS receivers. Finally, conclusions are given in Section 6.

2. HARDWARE DESIGN

The proposed receiver is composed of two main stages: a multi-band GNSS RF front-end, and a digital signal processing platform, which are described in the following.

2.1 RF Front-end

The RF front-end is designed to operate simultaneously with the L1 and L2 bands of GPS and GLONASS. Fig.1 is a simplified block diagram of the proposed RF front-end that is based on the previous work presented in [1].

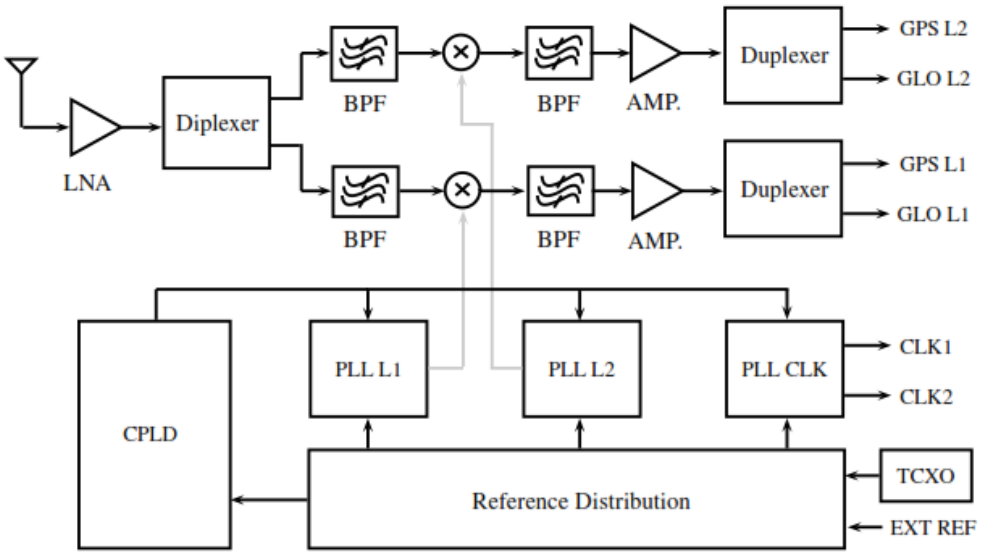

Figure 1. Simplified block diagram of the RF front-end.

The first stage of the front-end is a wideband low noise amplifier (LNA) that sets the noise figure of the receiver. The design of the LNA is based on a low noise transistor and it is implemented with discrete components. The measured noise figure of the LNA is about 1.1 dB; therefore the front-end has a high sensitivity, which is needed for high precision GNSS applications [2].

Due to the frequency bands of interest being separated about 300 MHz, to simplify the design, the RF signals are divided by a diplexer. This creates two channels, one for the L1 band and another for the L2 band. In order to select the desired bands, proper filtering is applied in each channel. In particular, surface acoustic wave band-pass filters (BPF) are used. Then, the bands are down-converted to an intermediate frequency (IF) by mixing the signals with local oscillators (LO). Active mixers are used because of the gain requirement of the front-end, which is high since the received signals are weak.

After the mixers, band-pass filters implemented with discrete components are placed to reject the unwanted mixing products. To obtain the gain needed to drive the analog to digital converters (ADC) of the digital signal processing platform we use MMIC IF amplifiers. Finally, since the GPS and GLONASS signals are located in different frequency bands, we separate the GPS and GLONASS bands in each channel before addressing digitalization. With this architecture, a significant reduction of the sampling rates can be achieved, simplifying the digital signal processing platform in relation to the processing requirements, storage of information and power consumption. The GPS and GLONASS bands separation is accomplished by means a duplexer, basically composed by a low-pass filter and a complementary high-pass filter. These duplexers also set the bandwidth of each band of the receiver, which is around 10 MHz. In the proposed design, the duplexers are implemented with discrete components.

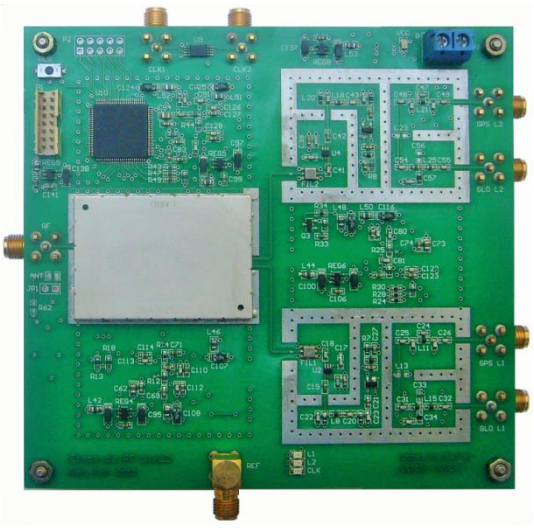

Figure 2.a. Implemented receiver RF front-end.

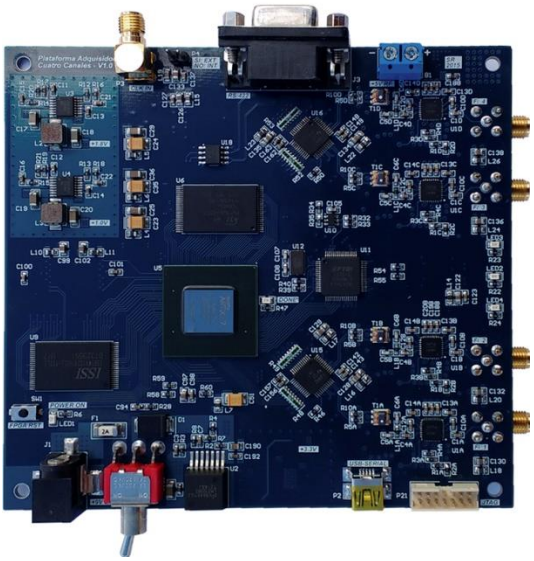

Figure 2.b. Digital Signal Processing Platform

Both local oscillators and the clock signal for the digital signal processing platform (CLK) are generated with frequency synthesizers based on phase locked loops (PLL) [2]. The three frequency synthesizers use the same frequency reference, which can be an internal temperature compensated crystal oscillator (TCXO) or an external oscillator for high precision applications. In the present design an external 10 MHz high stability oven controlled crystal oscillator (OCXO) is used. Fig.2, a) is a photo of the implemented prototype, which size is 10 cm x 12 cm.

2.2 Digital Signal Processing Platform

The digital signal processing platform is designed for processing four independent IF channels simultaneously. Fig.3 shows the block diagram of the current design, which was presented in a previous work [3]. The proposed design has an amplification stage, an analog to digital conversion stage and finally, a digital processing stage based on a FPGA with the associated interfaces (SRAM, FLASH memory and communications ports) needed for implementing ad-hoc hardware. The analog signals coming from the RF front-end are amplified by a variable gain amplifier (VGA). The FPGA allows developing a closed-loop system for controlling the gain. Two dual-channel 8-bit analog to digital converters (ADC) are used to digitize the analog signals. Each channel allows a maximum sample rate of 40 Msps with an analog bandwidth of 600 MHz, which is suitable for processing the signals of interest. The clock reference for the platform is obtained from the RF front-end and used by the FPGA to generate the ADC sample clock. This ensures coherent digital processing. To make the necessary GNSS signal correlations, a custom IP core is implemented in the FPGA using hardware description language. The entire digital processing system is controlled by a LEON 3 soft core implemented in the FPGA. The LEON 3 executes the receiver software loaded in FLASH memory. Because of the deterministic nature of the SRAM's access time, a real time operating system (RTOS) can be used, which is needed for critical applications. The platform has two communication interfaces, a USB port and a RS-422 interface that can be used to connect the receiver with specific equipment, like a navigation computer. Fig.2, b) is a photo of the implemented prototype, which size is 10 cm x 12 cm.

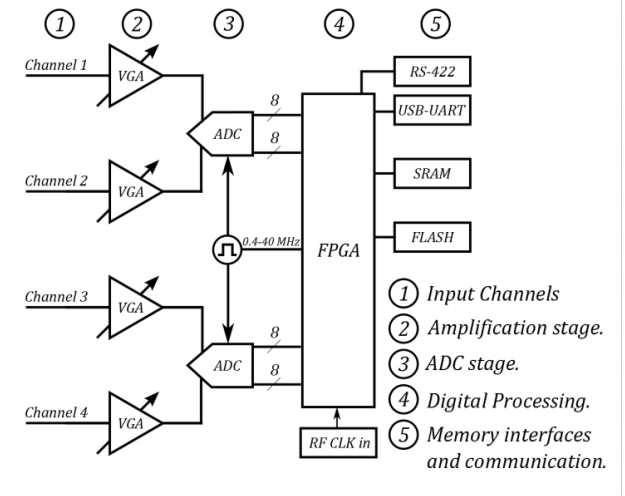

Figure 3. Simplified block diagram of the digital processing platform.

3. DIGITAL DESIGN DESCRIPTION

The digital design synthetized in the FPGA consists of 24 GPS/GLONASS correlation channels for tracking, a channel correlation for fast acquisition signal, a LEON3 microprocessor, a memory controller, multiple interface controllers for communication purpose and an automatic control gain module (AGC) as it is shown in Fig. 4a. The AGC adjusts the gain of the variable gain amplifiers (VGA`s) according to the level of samples received through the ADC's. The correlation channels receive the samples in intermediate frequency and correlate them with local replicas of the carrier and code signals. The correlation channels are designed to work as a co-processor and thus, to be controlled by the LEON3 microprocessor. This processor runs the software which must handle the correlator interruptions, read the results of the correlations and update the parameters of the channels for the next correlation interval, among other tasks. The AMBA bus is the interface that allows the processor to configure the correlation parameters of each channel independently and to control the rest of the peripherals.

A correlation channel for tracking is shown in Fig. 4b. Each of the tracking channels is configured independently through the AMBA bus interface. In this figure, three stages can be identified. In the carrier stage the generation of local replicas of carrier signal and a phase rotator are implemented. Look-up tables are used for generating sine and cosine trigonometric functions. The phase and frequency of the local carriers are controlled by a numerically controlled oscillator (NCO). The code stage consists of a C/A code generator that synthetizes the codes for all satellites of the GPS constellation and the code for GLONASS. A NCO controls the phase and frequency of the codes and a shift register allows configuring the delay between the seven code replicas with which the signal is correlated. The correlation stage does the sum or subtraction of the samples in-phase and in-quadrature coming from the phase rotator depending on the sign of the local code replicas. This occurs during the integration time controlled by a real time counter. When this time finishes, the results of the correlations of all replicas are stored in registers that are accessible from the AMBA bus for its reading by the LEON3.

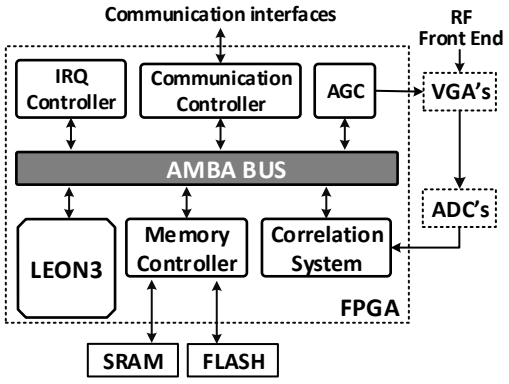

Figure 4.a Digital design architecture.

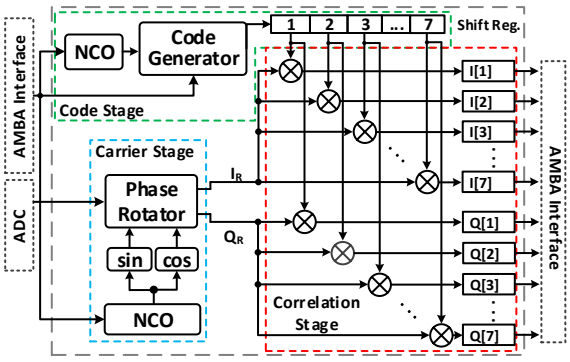

Figure 4.b Tracking correlation channel.

Unlike the tracking channels, the correlation channel for fast acquisition [5] correlates the signal with 20 code replicas with a fix delay between them. In this way, the satellite signal is acquired quickly with approximate values of carrier frequency and code delay in the acquisition stage and then, in the tracking stages, these parameters are adjusted more accurately.

4. SOFTWARE DESIGN

The higher levels of signal processing are performed by the system software that runs on the receiver's central processor. This piece of code is charged with performing mid-to-low level signal processing functions and measurement generation, to higher level navigation solution determination, while at the same time keeping tabs on the interface between the receiver and other external systems through communication channels, resource management, and system configuration.

The software is based on the real-time executive RTEMS, which provides a series of interfaces to perform low level system administration functions: task management, task synchronization, resource administration, low level communication interface drivers, etc. The receiver's software builds upon this foundation and adds a multitasked real-time application that is charged with performing all the application field specific processing algorithms: GNSS signal acquisition and tracking, navigation message decoding, navigation solution determination, orbit prediction, correlation hardware resources administration, communication, etc. At its core, the software must interact with the low-level GNSS signal correlation hardware in order to process the incoming GNSS satellite's signal transmissions and generate pseudorange and deltarange measurements. This is a very intensive process that takes most of the CPU cycles, and is divided in two types of signal processing: signal acquisition, and signal tracking.

Signal acquisition is the process by which the receiver discovers a GNSS satellite signal present on the antenna, and establishes a coarse approximation of the most important signal parameters: carrier frequency, spreading code phase, and bit synchronization information. The receiver can only perform a single acquisition process at any given time, so multiple satellite acquisitions must be serialized on time. Once a GNSS satellites transmission has been acquired, this signal is put on tracking. Tracking is the process by which the receiver continuously updates its best estimate of the signal's parameters using a set of closed-loop phase-tracking and delay-tracking loops. The receiver can keep up to 24 GPS/GLONASS signals on tracking simultaneously, or up to 12 GPS L1/L2 signals, depending on the bands of interest of a particular implementation. Both signal acquisition and signal tracking algorithms have been specifically tailored to cope with the kind of signal distortions typical for the dynamics of a vehicle in low earth orbit: high speed and constant acceleration. The acquisition search domain has been broadened to account for high signal carrier deviations caused by Doppler Effect, and the phase-tracking loops use a fourth order, type three, loop filter to achieve zero stationary error on constant vehicle acceleration.

The signal parameters are used to build pseudorange and deltarange measurements for each of the satellites kept on tracking. These measurements are passed on to the navigation module, where they are processed to determine the PVT (Position, Velocity and Time) navigation solution once every second. This navigation solution and multiple other pieces of information are transmitted through the communication channels using a simple RS-422 port on the receiver board, with a proprietary transmission protocol.

5. PERFORMANCE TESTS

To analyze the performance of the measurements of pseudorange, delta-range and carrier phase provided by the receiver, we carried out a test in a controlled scenario. For that, we used a high-fidelity GNSS signal generator where we configured a static receiver position and a signal power that produces a C/N0 of 45dB/Hz at the receiver (for all the satellites in view),obtaining the pseudorange, delta-range and carrier phase observables. Based on the generator data, we can determine the true range and range-rate for each satellite, $\widehat{\rho}_{kj}$ and $\widehat{\dot{\rho}}_{kj}$ and obtain the difference between the measurements and the real data, called measurement residuals.

$$\breve{\rho}_{kj} = \rho_{kj} - \widehat{\rho}_{kj} = b_k + \nu_{kj} \tag{1}$$

$$\breve{\dot{\rho}}_{kj} = \dot{\rho}_{kj} - \widehat{\dot{\rho}}_{kj} = \dot{b}_k + \upsilon_{kj} \tag{2}$$

Since the measurements are affected by the clock bias and clock drift, b_k and $\dot{b}_k$ (as can be seen in the model presented in [5] and [6]), these terms remain in the residuals. To eliminate these effects we take the so called simple difference between two residuals – i.e. the difference between the residuals of two satellites. In absence of other error terms, the simple difference of residuals contain the difference of terms due to the noise that affect the measurements, i.e. a noise term with a variance that is the sum of both variances, assuming statistical independence.

$$\Delta\breve{\rho}_{kj} = \breve{\rho}_{kj} - \breve{\rho}_{kj_0} = \nu_{kj} - \nu_{kj_0} \tag{3}$$

$$\Delta\breve{\dot{\rho}}_{kj} = \breve{\dot{\rho}}_{kj} - \breve{\dot{\rho}}_{kj_0} = \upsilon_{kj} - \upsilon_{kj_0} \tag{4}$$

In Fig. 5 we present the simple difference results obtained in the test. As can be seen, for each simple difference we can obtain a variance estimation. If we define the variance estimation as the mean of these different estimates, we obtain (we also include the results for phase measurements, whose estimation in similar to the presented)

$$\hat{\sigma}_\rho = \frac{1}{12 \cdot 11} \sum_{j_0} \sum_{j} \hat{\sigma}_{\rho,j} = 1{,}14 \times 10^{-1} \text{ [m]} \tag{5}$$

$$\hat{\sigma}_{\dot{\rho}} = \frac{1}{12 \cdot 11} \sum_{j_0} \sum_{j} \hat{\sigma}_{\dot{\rho},j} = 2{,}98 \times 10^{-2} \text{ [m/s]} \tag{6}$$

$$\hat{\sigma}_\phi = \frac{1}{12 \cdot 11} \sum_{j_0} \sum_{j} \hat{\sigma}_{\phi,j} = 6{,}85 \times 10^{-4} \text{ [m]} \tag{7}$$

As a comparison, consider the values provided in the datasheet of PolaRx5 receiver by Septentrio. The unfiltered GPS pseudorange error is 0.16m, the carrier frequency error

1.9cm/s, and the carrier phase error 1mm [7]. Excepting the carrier frequency error - which was not particularly optimized in the design- our receiver presents better results than the ones of this well-known reference GNSS receiver.

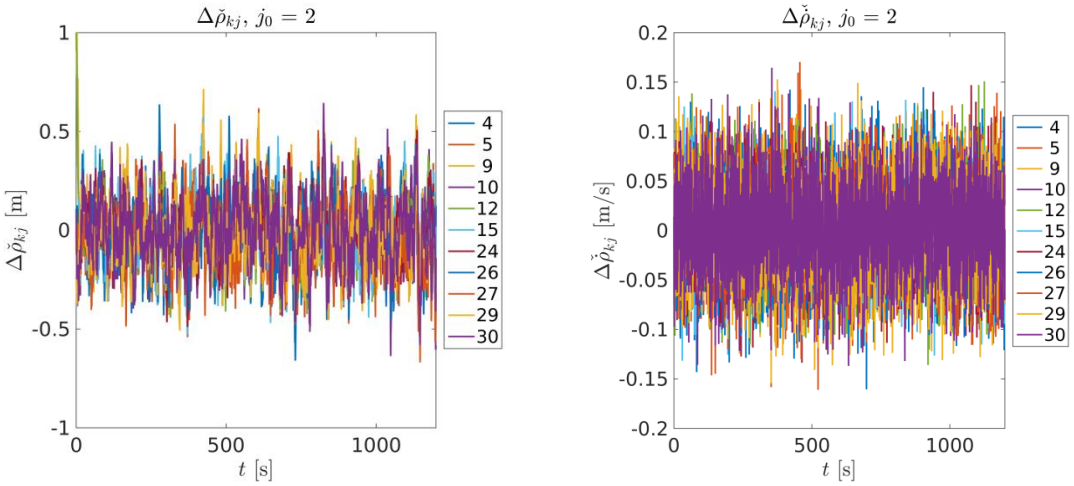

Figure 5. Pseudorange (left) and delta-range (right) measurements residuals simple differences, taking the measurement of satellite 2 as reference.

6. CONCLUSIONS

The different aspects of the architecture and design of a new GNSS receiver intended for small satellite applications, completely conceived in Argentina, has been presented. A prototype of the GNSS receiver has been built and experimentally tested with a GNSS signal simulator showing the excellent quality of the raw measurements produced. In particular, the performance of the pseudorange errors obtained is less than 12 cm, and less than 0.7 mm in the carrier phase. These results are on a level with the best high precision GNSS receivers utilized nowadays in surveying applications and show clearly the high potential of the receiver for absolute and relative orbit determination.

7. REFERENCES

[1] G. Ramón López La Valle, Javier G. García, P. Agustín Roncagliolo y Carlos H. Muravchik, An L1 or L2 Multi-Constellation GNSS Front-End for High Performance Receivers, Journal of Surveying and Mapping Engineering, vol. 1, no. 3, pp. 56-64 (2013).

[2] G. Ramón López La Valle, Cabezal de RF de un Receptor GNSS Multibanda, M.S. thesis, Universidad Nacional de La Plata, Argentina (2014).

[3] Santiago Rodríguez, Ramón López La Valle, Pedro A. Roncagliolo y Javier G. García, Plataforma de adquisición y procesamiento digital de cuatro canales, in proc. AADECA 2016, Buenos Aires (2016).

[4] J. G. Díaz, P. A. Roncagliolo, J. G. García, Canal de correlación de adquisición no-coherente GPS/GLONASS, XV Reunión de Trabajo en Procesamiento de la Información y Control - RPIC 2013, pp. 445-450, S. C. de Bariloche, Río Negro, Argentina.

[5] E. Kaplan and C. Hegarty, Understanding GPS: Principles and Aplications, Artech House (2005)

[6] B. Hofmann-Wellenhof, H. Lichtenegger, and E. Wasle, GNSS - Global Navigation Satellite Systems: GPS, GLONASS, Galileo, and more, Springer (2007).

[7] Septentrio, PolaRx5 Multi-frequency GNSS Reference Receiver Specifications, 2015.